Stationary and drifting localized structures near a multiple bifurcation point

Yu. A. Logvin,[1,2] B. Schäpers,[2] and T. Ackemann[2]
[1]*Institute of Physics, Academy of Sciences, Skaryna avenue 70, 220072 Minsk, Belarus*
[2]*Institut für Angewandte Physik, Westfälische Wilhelms-Universität Münster, Corrensstraße 2/4, D-48149 Münster, Federal Republic of Germany*

(Received 19 July 1999)

Localized states embedded in a patterned background are found in numerical simulations of spontaneous pattern formation in a spin-1/2 atomic system with optical feedback. In the vicinity of a parameter region with bistability between two homogeneous states large amplitude peaks as well as dark holes exist as stable localized states on a hexagonal background. Moreover, resonant interaction between oscillatory and stationary inhomogeneous modes produces a nonstationary background which may force the localized states to drift.

PACS number(s): 47.54.+r, 42.65.Sf, 82.40.Bj

Multistability of several states in a spatially extended nonlinear system may result in the appearance of localized structures when a pattern is embedded in a background corresponding to a different state. The best known objects are localized states (LS) [1–3], which in different treatments were named also autosolitons [4,5], spatial solitons [6], or ‘‘optical bullet holes’’ [7] in an optical context. In most cases considered so far, the LS exist on a homogeneous background. Bistability between different inhomogeneous states can result in the formation of localized patterns (LP). These can have the form of large area regions with different patterns, which are separated by domain boundaries [8–13]. More recently also the existence of small localized patches of one pattern or even single peaks embedded in a background corresponding to another pattern was demonstrated [14,9,10,15–17].

An experimental demonstration of the latter case (large amplitude solitary peaks superimposed on a small amplitude hexagonal lattice) was recently given in an optical system [16]. The observations were related to the simultaneous occurrence of a modulational instability and bistability between two homogeneous states. In this paper, we are going to investigate theoretically a related optical system in more detail, in which different (stationary and nonstationary) periodic patterns exist close to a region with bistability between homogeneous states and may serve as a background for LS's. These different background patterns can be selected by tuning a single stress parameter.

In our system, pattern formation is due to the nonlinear interaction of an intense light field with sodium vapor in an external magnetic field. The transmitted light is fed back into the vapor by a distant plane reflector (cf. Fig. 1). During the propagation to the mirror and back different points in the transverse cross section of the beam are coupled by diffraction. The interaction between the vapor and the light can be controlled in a wide range by parameters such as the light frequency or the magnetic field which are easily accessible in experiments. In this paper the parameters are chosen to obtain different overlapping instabilities: modulational instabilities which generate periodic patterns of different length scales, bistability of the homogeneous state, and a pattern-forming Hopf instability. The physical reason for the latter instability is the Larmor precession of the magnetization of the Na atoms.

Since the system is already described in the literature [18–23], we omit here the detailed description. The pattern formation processes are described with the help of the quantum mechanical equation of motion for the Bloch vector $\boldsymbol{m}=(u,v,w)$, representing the magnetization of the spin-1/2 sodium ground state [18,19]:

$$\partial_t \boldsymbol{m}=-(\gamma-D\Delta_\perp+P)\boldsymbol{m}-\boldsymbol{m}\times\boldsymbol{\Omega}+\hat{\boldsymbol{e}}_{\boldsymbol{z}}P \tag{1}$$

and the classical paraxial wave equation for the light propagation [24]. In Eq. (1), γ is the collision induced relaxation of $\boldsymbol{m}$, D is the diffusion constant, $\Delta_\perp$ is the transverse part of the Laplacian, P denotes the optical pump rate. The vector $\boldsymbol{\Omega}=(\Omega_x,0,\Omega_z-\bar{\Delta}P)$ is a torque vector, whose components are given by the Larmor frequencies corresponding to the Cartesian components of the external magnetic field and the light-shift induced level shift $\bar{\Delta}P$. $\bar{\Delta}$ is the detuning between the incident field and the atomic transition, normalized to the homogeneous linewidth Γ_2 (half width at half maximum). The pump rate P is taken to be proportional to the sum of the intensities of the forward (E_0) and the backward (E_b) waves:

$$P=(|E_0|^2+|E_b|^2)\frac{|\mu_e|^2}{4\hbar^2\Gamma_2(\bar{\Delta}^2+1)}, \tag{2}$$

where μ_e denotes the dipole matrix element of the transition. The backward field is related to the incident one by

$$E_b=\sqrt{R}e^{-id\Delta_\perp/k_0}e^{-i\chi_{\mathrm{lin}}(1-w)k_0l/2}E_0, \tag{3}$$

where the first exponential factor results from the formal solution of the paraxial wave equation describing the light propagation over the distance $2d$ between the cell and the mirror (reflection coefficient R) and back. The second expo-

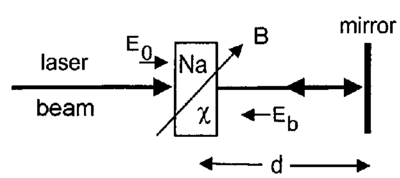

FIG. 1. Schematic diagram of the considered optical system.

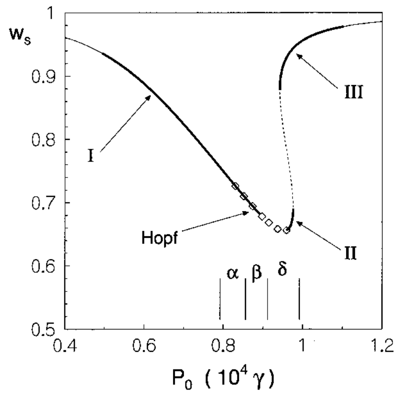

FIG. 2. Steady-state orientation w versus external pump rate for the parameters $\overline{\Delta}=8$, $R = 0.915$, $l=15$ mm, $\Omega_z/2\pi=100$ kHz, $\Omega_x/2\pi=9$ kHz, $d=100$ mm, and $D=180$ mm^2/s. The intervals with formation of stationary patterns are marked by thick solid lines and diamonds (Hopf instability). The intervals I and II are separated near the minimum of the nonlinear resonance where only Hopf modes are unstable. The interval III is not essential for the matter of this paper. Domains α, β, and δ correspond to different types of localized patterns.

nential factor is responsible for the light propagation within the nonlinear medium with a susceptibility $\chi_{\rm lin}(1-w)$. k_0 is the wave number of light in vacuum, l is the length of the nonlinear medium [25]. As a control parameter we consider the pump rate P_0 introduced by the forward beam ($P_0 \sim |E_0|^2$).

In our situation, pattern formation takes place under specific conditions, as it can be seen from the steady state characteristic (SSC) in Fig. 2, where the steady homogeneous solution w is plotted versus P_0. A bistable characteristic occurs when a specific condition of nonlinear resonance is fulfilled, i.e., the action of the longitudinal external field is ''cancelled'' by the light induced level shift ($\Omega_z \approx \overline{\Delta} P$) [22]. Regions of the SSC where the homogeneous steady state is unstable against perturbations by spatially dependent static (denoted by I, II, and III in Fig. 2) or Hopf modes are depicted by thick solid lines or diamonds, respectively. The spatial wave numbers of the structures due to the Hopf instability and the static-II instability are approximately the same, while the static-I instability produces a structure whose wave number is about 1.7 times larger than the former ones. As a result, resonant interaction of these modes occurs when the sum of the wave vectors of the modes with smaller wave numbers is in resonance with a mode with a larger wave number. This is the reason for a secondary instability from hexagons to *ultrahexagons* [18,20] and for the emergence of *winking* hexagons [21] in our system.

Carrying out simulations in the vicinity of the minimum of the nonlinear resonance we have found different domains (α,β,δ in Fig. 2) where different kinds of localized structures occur. The results of numerical simulations have been verified using different integration schemes (explicit, hopscotch, alternating-direction-implicit integration) to treat the Laplacian term in the Bloch equations. The diffraction operator has been treated with a spectral method and a fast Fourier transform. Periodic boundary conditions have been imposed. Most of the simulations have been carried out using a grid of 128×128 points, but all results discussed in this article have been cross-checked on a larger grid with 512×512 points. Below we describe the results of numerical simulations and discuss the developed spatial structures on the basis of a linear stability analysis.

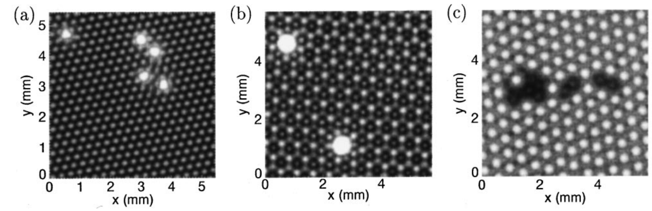

FIG. 3. (a) Localized pattern from the α domain of Fig. 2 demonstrating stable bright localized states on the static hexagonal background. (b) A snapshot of localized states on the nonstationary winking hexagon background from the β domain of Fig. 2. (c) Localized pattern from the δ domain demonstrating black holes on the background of positive hexagons. The white regions in (a) and (b) are overexposed in order to emphasize the background.

α domain. If we increase the control parameter P_0 up to the level of the α domain in Fig. 2 static positive hexagons emerge out of the random initial noise. We will refer to these hexagons as small-scale ones, because their wavelength is smaller than that of the structures due to the other instabilities. These small-scale stationary hexagons are stable almost in the whole interval where the homogeneous state is also unstable versus the Hopf bifurcation. We are able to produce bright peaks on the background created by these stationary small-scale hexagons by increasing the parameter P_0 for a short period in arbitrarily chosen domains of the transverse grid. Figure 3(a) shows the transverse distribution of the orientation w resulting from this simulation. A comparison of the amplitudes of these peaks with the SSC in Fig. 2 reveals a localized switching to a state close to the upper bistable state. (Note that the upper homogeneous state does not exist for these parameters, but as it has been discussed quite recently [26,27], the interaction between the homogeneous mode and the pattern forming mode in the vicinity of an interval of bistability can create additional homogeneous solution branches and thus can effectively widen the bistability domain.) Illumination with a rather broad transverse perturbation does not produce a spatially smooth state, but several bright peaks appear which can form amorphous clusters without an internal order, like those presented in the central part of Fig. 3(a). Comparing the profile of a localized structure with the profile of a constituent of the hexagonal pattern belonging to instability region II [similar to Fig. 3(c)] we find that they virtually coincide from the peak to the background of the hexagonal constituents. However, the background is considerably lower for LS in the α domain. Therefore we conclude that the bright large amplitude peaks in Fig. 3(a) are due to a manifestation of the static-II instability. Concluding the discussion of the α domain we note that the main characteristics of the LP here are as follows: The patterns are stationary and the background for large amplitude peaks is a small-scale positive hexagonal pattern.

β-domain. In this case, the background for LS is a nonstationary pattern produced by resonant interaction of the static-I and Hopf instabilities. As discussed in Refs. [21,23], the sum of the wave vector of two Hopf modes with tempo-

ral frequencies Ω and $-\Omega$ and spatial wave number k can coincide with the wave vector of a static mode with a spatial wave number $q=\sqrt{3}k$. A pattern created by two resonantly coupled hexagonal triads of static and Hopf modes has been named *winking* hexagons [21] and was obtained in numerical simulations starting from suitable initial conditions.

In Fig. 3(b) an example of a localized large amplitude peak on a background created by winking hexagons is shown. As in the α domain, these LS have been created numerically by a local increase of P_0 for a short period of time. The peaks seem to be of the same origin as the ones in Fig. 3(a). The main change is the type of the background pattern. Therefore the structures appearing in the β domain are classified as localized peaks appearing on a background of nonstationary hexagons.

The image in Fig. 3(b) is only a snapshot. Together with the oscillating small amplitude constituents forming the winking hexagons the large amplitude peaks drift on the background, however, with a very small velocity (compared to the oscillatory dynamics of the background). We associate this slow time scale of the drift motion with the small relaxation constant γ (of the order of s^{-1}) while the Hopf frequency is of the order of the Larmor frequency (tens of kHz). It is well known that the sum of the phases of the modes composing the principal hexagon triad is a main characteristic for hexagonal structures. For ideal positive and negative hexagons this sum is 0 and π, respectively. [The sum equal to 0 corresponds to the case of the small-scale hexagons in Fig. 3(a).] Typically the phase sum of the Hopf modes is not constant over the whole transverse area, e.g., in Fig. 3(b) there is a gradient in a nearly vertical direction. We have found in simulations that the drift motion of the large amplitude localized state roughly coincides with the direction of the sum phase gradient. This matches the long-known fact that in optical systems, in which the optical field is itself the dynamical variable, a phase gradient causes a drift of the LS [7,28]. Our result indicates that gradients in the dynamical variable will favor a drift independently of the nature of the physical variable.

Along with winking hexagons (elements of which are traveling waves), we have also observed in the β domain the formation of a nonstationary hexagon background composed of three standing waves. Again, the Hopf modes have been obtained to be in resonance with the static-I modes. In a recent numerical study of a Swift-Hohenberg equation, Brand and Deissler obtained hexagons built from three standing waves and referred to such nonstationary patterns as *blinking* hexagons [29]. Brand and Deissler do not investigate the structures in Fourier space of the developed patterns. Therefore it is not possible do decide whether the pattern they observe coincides with ours, i.e., whether they also contain the small scale ''harmonic'' static hexagons.

We have carried out numerical simulations for the case of one spatial transverse dimension and found that the traveling and standing waves emerging due to the pattern-forming Hopf instability coexist in the β domain. Also, formation of LS has been obtained on a background consisting of traveling as well as standing waves. The nonstationary hexagons composed of three traveling or standing waves are a natural generalization of the one-dimensional waves for the case of two transverse dimensions. In view of the recent study of bistability between traveling and standing waves in a generalized complex Swift-Hohenberg equation [30], it is not surprising that we observe bistability between different kinds of nonstationary hexagons. In simulations, the visual difference between them is that in the case of the *winking* hexagons, the same pattern appears shifted in the transverse plane after 1/3 and 2/3 of the oscillation period, whereas a standing pattern only reproduces itself after the full oscillation period.

δ domain. At higher P_0 (δ domain, cf. Fig. 2) large amplitude hexagons create a background for localized patterns which are dark spots in this case. Figure 3(c) was calculated by starting the simulation with a perfect hexagonal pattern as the initial condition and decreasing the local intensity in some regions for a short period of time. Examining the transverse distribution of orientation we find that the offset level of the hexagonal lattice lies in the domain of the unstable branch of the characteristics in Fig. 2 and the dark spot tends to reach the lower bistable state. We believe that in this case the zero homogeneous mode determining the offset level of the hexagonal pattern is modified through interaction with the triad of roll (stripe) modes [26]. We verified the long-term stability of the structure in Fig. 3(c) over long integration times (comparable with γ^{-1}). However, this pattern shows some nonstationarity: The values of the maxima and the minima (as well as the intensity distribution within the dark spot) ''fluctuate'' slightly with time, although the whole pattern remains structurally stable. Whether this nonstationarity is a residual action of the Hopf instability, or whether it is due to the internal complexity of the pattern is an open question at this stage of investigation.

In conclusion let us compare our findings with the results known in the field of pattern formation. Coexistence of domains of different patterns is a rather widely observed phenomenon [8,9,31]. In this context, the excitation of a single localized state on a hexagonal background is rather rare and it is interesting to note that similar phenomena have been experimentally observed recently in a nonlinear optical experiment [16]. The two-dimensional geometry and resonant interaction between different instabilities make the dynamics in our system especially sophisticated and the possible structures very numerous. Compared to other cases where static localized structures were studied in the vicinity of a saddle-node bifurcation (bistability) of the homogeneous mode [6,27,16], we note that in our case the Hopf instability brings about new delicate features.

[1] S. Koga and Y. Kuramoto, Prog. Theor. Phys. **63**, 106 (1980).
[2] O. Thual and S. Fauve, J. Phys. (France) **49**, 1829 (1988).
[3] R. J. Deissler and H. R. Brand, Phys. Rev. Lett. **74**, 4847 (1995).
[4] B. S. Kerner and V. V. Osipov, *Autosolitons: A New Approach to Problems of Self-Organization and Turbulence* (Kluwer, Dodrecht, 1994).
[5] N. N. Rosanov, *Progress in Optics XXXV*, edited by E. Wolf (Elsevier, Amsterdam, 1996), p. 1.
[6] M. Brambilla, L.A. Lugiato, F. Prati, L. Spinelli, and W. J.

Firth, Phys. Rev. Lett. **79**, 2042 (1997).
[7] W. J. Firth and A. S. Scroggie, Phys. Rev. Lett. **76**, 1623 (1996).
[8] J. Hegseth, J. M. Vince, M. Dubois, and P. Bergé, Europhys. Lett. **17**, 413 (1992).
[9] S. Residori, P. L. Ramazza, E. Pampaloni, S. Boccaletti, and F. T. Arecchi, Phys. Rev. Lett. **76**, 1063 (1996).
[10] M. Meixner, A. De Wit, S. Bose, and E. Schöll, Phys. Rev. E **55**, 6690 (1997).
[11] G. D. Granzow and H. Riecke, Phys. Rev. Lett. **77**, 2451 (1996).
[12] A. J. Scroggie, W. J. Firth, G. S. McDonald, M. Tlidi, R. Lefever, and L. A. Lugiato, Chaos, Solitons and Fractals **4**, 1323 (1994).
[13] M. Tlidi, P. Mandel, and M. Haelterman, Phys. Rev. E **56**, 6524 (1997); M. Tlidi, P. Mandel, and R. Lefever, Phys. Rev. Lett. **73**, 640 (1994).
[14] S. V. Fedorov, G. V. Khodova, and N. N. Rosanov, Proc. SPIE **1840**, 208 (1991).
[15] D. Raitt and H. Riecke, Phys. Rev. E **55**, 5448 (1997).
[16] A. Schreiber, B. Thüring, M. Kreuzer, and T. Tschudi, Opt. Commun. **136**, 415 (1997).
[17] M. Tlidi and P. Mandel, Phys. Rev. A **59**, R2575 (1999).
[18] T. Ackemann, Yu. A. Logvin, A. Heuer, and W. Lange, Phys. Rev. Lett. **75**, 3450 (1995).
[19] W. Lange, Yu. A. Logvin, and T. Ackemann, Physica D **96**, 230 (1996).
[20] Yu. A. Logvin, T. Ackemann, and W. Lange, Phys. Rev. A **55**, 4538 (1997).
[21] Yu. A. Logvin, T. Ackemann, and W. Lange, Europhys. Lett. **38**, 583 (1997).
[22] T. Ackemann, A. Heuer, Y. A. Logvin, and W. Lange, Phys. Rev. A **56**, 2321 (1997).
[23] Yu. A. Logvin and T. Ackemann, Phys. Rev. E **58**, 1654 (1998).
[24] W. J. Firth, J. Mod. Opt. **37**, 151 (1990); G. D'Alessandro and W. J. Firth, Phys. Rev. A **46**, 537 (1992).
[25] We neglect diffraction effects inside the cell, supposing the cell to be very thin in comparison with the length between the cell and the mirror.
[26] S. Métens, G. Devel, P. Borckmans, and R. Engelhardt, Europhys. Lett. **37**, 109 (1997).
[27] D. Michaelis, U. Peschel, and F. Lederer, Phys. Rev. A **56**, R3366 (1997).
[28] V. B. Taranenko, K. Staliunas, and C. O. Weiss, Phys. Rev. A **56**, 1582 (1997).
[29] H. R. Brand and R. J. Deissler, Phys. Lett. A **231**, 179 (1997).
[30] V. J. Sánchez-Morcillo, G. J. de Valcárcel, E. Roldán, and K. Staliunas, Phys. Rev. E **57**, R4911 (1998).
[31] M. C. Cross and P. C. Hohenberg, Rev. Mod. Phys. **65**, 851 (1993).